Proc. Natl. Acad. Sci. USA
Vol. 93, pp. 5307–5312, May 1996
Genetics

Adenine phosphoribosyltransferase-deficient mice develop 2,8-dihydroxyadenine nephrolithiasis

(purine metabolism/gene targeting/mouse model/renal disease)

SANDRA J. ENGLE*, MICHAEL G. STOCKELMAN†, JU CHEN*, GREG BOIVIN‡, MOO-NAHM YUM§, PHILIP M. DAVIES¶, MO YIN YING†, AMRIK SAHOTA*, H. ANNE SIMMONDS¶, PETER J. STAMBROOK†, AND JAY A. TISCHFIELD*‖

*Departments of Medical and Molecular Genetics, and §Pathology and Laboratory Medicine, Indiana University School of Medicine, 975 West Walnut Street, Indianapolis, IN 46202-5251; †Departments of Cell Biology, Neurobiology, and Anatomy, and ‡Pathology and Laboratory Medicine, University of Cincinnati College of Medicine, Cincinnati, OH 45267; and ¶Purine Research Laboratory, Guy's Hospital, London, SE1 9RT, United Kingdom

Communicated by Frank H. Ruddle, Yale University, New Haven, CT, February 8, 1996 (received for review December 4, 1995)

ABSTRACT **Adenine phosphoribosyltransferase (APRT) deficiency in humans is an autosomal recessive syndrome characterized by the urinary excretion of adenine and the highly insoluble compound 2,8-dihydroxyadenine (DHA) that can produce kidney stones or renal failure. Targeted homologous recombination in embryonic stem cells was used to produce mice that lack APRT. Mice homozygous for a null *Aprt* allele excrete adenine and DHA crystals in the urine. Renal histopathology showed extensive tubular dilation, inflammation, necrosis, and fibrosis that varied in severity between different mouse backgrounds. Thus, biochemical and histological changes in these mice mimic the human disease and provide a suitable model of human hereditary nephrolithiasis.**

Adenine phosphoribosyltransferase (APRT; EC 2.4.2.7) is a ubiquitously expressed enzyme that catalyzes the synthesis of adenosine monophosphate from adenine and 5-phosphoribosyl-1-pyrophosphate (1). Adenine is produced endogenously as a by-product of the polyamine pathway and by the reaction of adenosine with *S*-adenosylhomocysteine hydrolase (2, 3). In the absence of functional APRT, adenine is oxidized by xanthine dehydrogenase (XDH; EC 1.2.3.2), by an 8-hydroxy intermediate, to 2,8-dihydroxyadenine (DHA) (4). The sparingly soluble nature of DHA at the normal pH of human urine (5) results in the excretion of DHA crystals in the urine and, frequently, the deposition of DHA stones in the kidneys. Adenine, which is not normally found in the urine at detectable levels, is also excreted.

Clinical symptoms of APRT deficiency vary from benign to life-threatening and may be present from birth or have onset late in life (reviewed in ref. 1). Symptoms include crystalluria, colic, hematuria, dysuria, recurrent urinary tract infections, and kidney stones. Some patients may progress to acute or chronic renal failure, necessitating maintenance dialysis or kidney transplant(s) (6, 7). All other biochemical and hematological parameters in APRT-deficient patients appear to be normal.

APRT deficiency is inherited in an autosomal recessive manner, consistent with the localization of the single-copy gene to 16q24 (8). Heterozygous carriers are usually unaffected, although one affected heterozygous male has been reported (9). The frequency of heterozygosity for APRT deficiency has been estimated by several studies to be 0.4–1.2% (10–12). This estimate suggests that a much larger population of homozygous individuals exists than the ≈100 patients that have been identified in the North American, European and Middle Eastern populations. It has been suggested that asymptomatic and misdiagnosed patients may account for some of the unidentified homozygotes and/or that APRT deficiency may sometimes be lethal *in utero* (1, 13).

Characterization of the natural course and clinical variation of APRT deficiency has been extremely difficult because of a lack of readily accessible affected individuals and their families. Although studies of animals and humans treated with adenine or DHA (14–17) have provided some useful information, they do little to address the questions posed by the chronic adenine excess and DHA production seen in hereditary APRT deficiency. Therefore, we generated an APRT-deficient mouse via targeted homologous recombination in mouse embryonic stem (ES) cells.

MATERIALS AND METHODS

Gene Targeting. The targeting vector was constructed from a 5.6-kb *Aprt*-containing genomic DNA fragment isolated from a single λ phage clone isolated from a mouse DNA library (strain 129/Sv, kindly provided by M. Shull, University of Cincinnati College of Medicine). An *Xho*I–*Sal*I fragment containing the neomycin resistance cassette from pMC1NeoPolyA (Stratagene) was introduced, in the same transcriptional orientation as *Aprt*, into a unique *Bsp*EI site in exon 3. A herpes simplex virus thymidine kinase gene cassette driven by a modified thymidine kinase promoter containing two polyoma enhancer sequences was introduced, in the same transcriptional orientation as *Aprt*, into a *Bsm*I site 1.5 kb 3′ of the *Aprt* termination codon.

D3 ES cells (18) derived from strain 129/Sv mice were cultured on mitomycin C-treated embryonic fibroblast feeder layers or on gelatin-coated dishes in Buffalo rat liver (BRL)-conditioned or leukemia inhibitory factor (LIF)-supplemented medium, essentially as described (19). LIF was from Life Technologies (Grand Island, NY). Exponentially growing ES cells (3×10^6 or 5×10^6) were resuspended in 1 ml of electroporation buffer (20 mM Hepes, pH 7.05/137 mM NaCl/5 mM KCl/0.7 mM Na_2HPO_4/6 mM glucose/1 mg/ml bovine serum albumin/0.1 mM β-mercaptoethanol) containing 10 μg of the targeting vector (MBSF18) linearized at a unique *Ssp*I site in the pUC19 vector. Electroporation was performed in a Cell-Porater (Life Technologies) at 200 V, 1180 μF, at room temperature. Cells were incubated for 10 min at room temperature before reseeding on 10-cm gelatin-coated culture dishes at a density of 3×10^5 or 5×10^5 cells per dish in BRL-conditioned or LIF-supplemented medium. G418 selection (200 units/ml; Life Technologies) was begun 48 hr after electroporation and ganciclovir selection (0.2 mM; courtesy of Syntex, Palo Alto, CA) was begun 96 hr after electroporation. After 7–10 days, colonies were isolated and expanded for 2–4 days in gelatin-coated 24-well dishes containing BRL-conditioned or LIF-supplemented medium. One-half of the cells were frozen, and the other half was expanded for DNA isolation.

Microinjection of ES cell into blastocysts was performed essentially as described (20). Blastocysts were collected from C57BL/6J females at 3 days post coitum, injected with 10–15

The publication costs of this article were defrayed in part by page charge payment. This article must therefore be hereby marked "*advertisement*" in accordance with 18 U.S.C. §1734 solely to indicate this fact.

Abbreviations: APRT, adenine phosphoribosyltransferase; DHA, 2,8-dihydroxyadenine; XDH, xanthine dehydrogenase; ES, embryonic stem; HPRT, hypoxanthine phosphoribosyltransferase.

‖To whom reprint requests should be addressed at: Department of Medical and Molecular Genetics, Indiana University School of Medicine, IB 130, 975 West Walnut Street, Indianapolis, IN 46202-5251.

targeted ES cells (MBSF1837), and reimplanted into pseudopregnant females. Male chimeric mice were mated to either C57BL/6J or Black Swiss females, and offspring were genotyped by Southern hybridization. Heterozygous mice were interbred to produce homozygous mice. Mice bred into a Black Swiss background were maintained in a pathogen-free barrier facility at the University of Cincinnati. Mice bred into a C57BL/6J background were similarly produced and maintained at Indiana University.

Southern Hybridization Analysis. High-molecular-weight genomic DNA was extracted from cell pellets using the method of Mullenbach and coworkers (21) and was extracted from mouse tails as described by Hogan and coworkers (20). Electrophoresis, and Southern blotting and hybridization were performed as previously described (22) with a final wash of 0.1× standard saline citrate (SSC)/0.5% SDS for 15 min at 42°C. Probe 1 corresponds to bases 106-1083 of the published mouse *Aprt* sequence, and probe 2 corresponds to bases 1870–2982 (23). Probe 3 corresponds to a *Hin*cII–*Bam*HI fragment located ≈1.8 kb 3′ of the *Aprt* stop codon. The membrane was exposed to autoradiography film (X-Omat AR, Eastman Kodak) for 24–96 hr.

Blood, Tissue, and Urine Collection. Blood was obtained from the orbital sinus of methoxyflurane (Mallinkrodt Veterinary, Mundelein, IL) anesthetized mice in heparinized blood-collecting Kimax capillaries (Curtin Matheson, Chicago). The blood was then transferred to a microcentrifuge tube and washed three times with 0.85% saline. Packed erythrocytes were frozen at −70°C before use. Tissues were removed from mice killed by cervical dislocation, quick frozen in dry ice or liquid nitrogen, and stored at −70°C. Before use, the tissues were homogenized in a small volume of extraction buffer (50 mM Tris·HCl, pH 7.4/5 mM $MgCl_2$) and centrifuged to remove cellular debris (13,000 rpm, 10 min). Urine was collected in microcentrifuge tubes and frozen at −70°C before analysis.

APRT Assay. Reactions involving erythrocyte lysates were typically carried out for 30 min at 37°C in a total volume of 50 μl of 55 mM Tris·HCl buffer, pH 7.4, containing 1 mM 5-phosphoribosyl-1-pyrophosphate (Na salt), 5 mM $MgCl_2$, 5 mg/ml bovine serum albumin, and ≈9 nM of 8-^{14}C-labeled adenine [≈50 mCi/mM (1 Ci = 37 GBq); DuPont/NEN or Amersham]. Liver extracts were assayed under the same conditions except that 1.1×10^{-2} M 3′-deoxythymidine 5′-triphosphate was included in the reaction mix. Reactions were terminated by the addition of 0.1 volume of 4 M $HClO_4$ followed by centrifugation (13,000 rpm, 5 min). Supernatants were transferred to fresh microcentrifuge tubes and incubated on ice for 20 min with 0.1 volume of 4 M KOH. After centrifugation (13,000 rpm, 5 min), ≈5 μl of supernatant was spotted on plastic-backed polyethyleniminecellulose TLC sheets (Baker), and the components were separated with water as the solvent. The sheets were dried, and the amount of radioactive substrate converted to product was determined by quantitation in an AMBIS β-scanner. The total protein concentration of the reaction was determined with the Bio-Rad Protein Assay Kit. The protein concentration was adjusted to yield between 15% and 50% conversion of substrate to product.

Analysis of Purine Metabolites in Urine. HPLC analyses were performed as described by Simmonds and coworkers (24). Nucleosides and bases were separated using a Millipore–Waters tri-module HPLC system and a prepacked Spherisorb 5 μm ODS analytical column (250 × 4.6 mm i.d.; Hichrom Ltd., Berks, U.K.) by linear gradient elution at room temperature using a flow rate of 1 ml/min. The linear gradient ran from 100% buffer A (40 mM ammonium acetate, pH 5.0) to 20% buffer B (80% methanol/10% acetonitrile/10% tetrahydrofuran, vol/vol) and absorbance was recorded at 254 and 280 nm with a full scale of 0.5 absorbance units with inline diode-array detection.

Pathology and Histopathology. Histological examination was performed on representative tissues from all major organ systems using an Olympus (New Hyde Park, NY) BX40 microscope. Tissues were fixed in 10% neutral buffered formalin, dehydrated through a gradient of alcohols, and embedded in paraffin. Sections (4 μm) were stained with hematoxylin and eoxin.

RESULTS

Production of APRT-Deficient Mice. A positive–negative gene targeting vector (25), MBSF18, was constructed from 5.6 kb of mouse genomic DNA (strain 129/Sv) containing the entire coding sequence of *Aprt* (Fig. 1). When this vector was electroporated into ES cells, 11 of 279 (3.9%) G418/gancyclovir-resistant clones contained one endogenous and one correctly targeted *Aprt* allele as determined by Southern hybridization analysis of *Eco*RI- or *Bst*EII-digested genomic DNA using probes 1, 2, and 3 (data not shown). Chimeric mice were produced by blastocyst injection (20) using one D3 ES cell clone, MBSF1837. Chimeric male mice were mated to either wild-type Black Swiss or C57BL/6J mice. Offspring generated from ES cell-derived sperm were tested for heterozygosity by Southern hybridization. Heterozygous mice, which all appeared phenotypically normal and healthy at 6 weeks of age, were sib-mated to produce homozygous mice. Black Swiss and C57BL/6J heterozygous mice were maintained at separate animal facilities and bred only with heterozygous animals of the same genetic background. Southern hybridization analysis was used to confirm the generation of homozygous mutant mice (Fig. 2).

Offspring of heterozygous mating pairs (239, 137 males and 102 females) were genotyped at 3–6 weeks of age. Of these, 27% was wild-type, 54% was heterozygous, and 19% was homozygous for the disrupted allele. χ^2 analysis indicates that the deviation from the expected values is only marginally significant ($P < 0.05$).

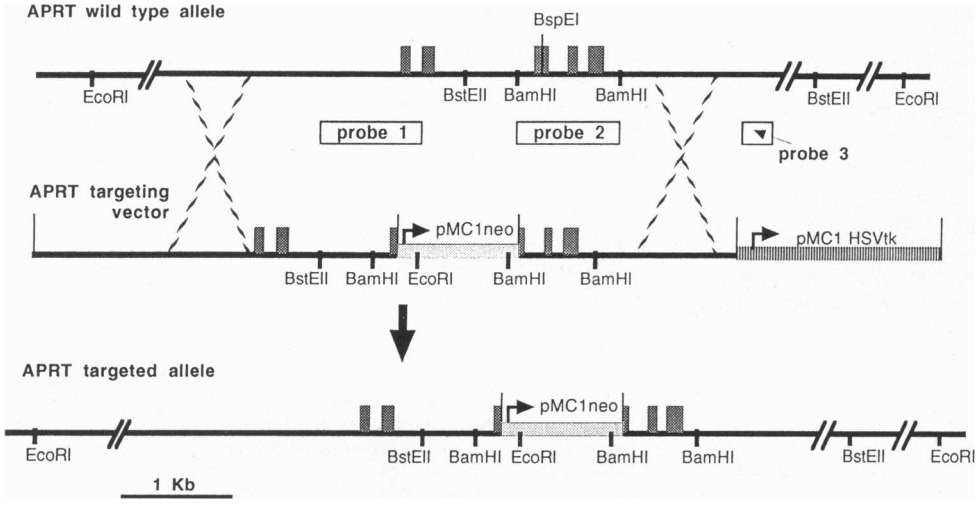

FIG. 1. Schematic representation of the *Aprt* targeting vector and recombination at the *Aprt* locus. A restriction map of wild-type *Aprt* is shown at the top of the diagram. Shaded boxes represent the five exons of *Aprt*. The probes used to detect diagnostic *Eco*RI, *Bst*EII, and *Bam*HI genomic DNA fragments are shown immediately below the line representing wild-type *Aprt*. The second line represents a restriction map of the *Aprt* targeting construct, MBSF18. Arrows indicate the transcriptional orientation of *neo* and herpes simplex virus *tk*. The third line represents the predicted structure of a mutated *Aprt* allele after homologous recombination.

Therefore, it is unlikely that APRT deficiency in mice is significantly lethal either *in utero* or before weaning.

To determine whether mice homozygous for the disrupted *Aprt* allele express any residual enzyme activity, APRT activity was assayed in erythrocyte lysates and liver extracts from wild-type, heterozygous, and homozygous mutant mice (Table 1). Homozygous mutant mice exhibit <1% of wild-type activity in both tissues. The disrupted *Aprt*, therefore, is a true null allele.

Heterozygous mice exhibit ≈32% and ≈22% of wild-type APRT activity in erythrocyte lysates and liver extracts, respectively. These values seem to support the hypothesis that only the APRT dimer composed of two wild-type subunits is stable and/or functional, and that all other dimer combinations are unstable and/or nonfunctional (26). Since the targeting vector was designed to produce a carboxyl-truncated protein, reverse transcription/PCR amplification was performed to confirm that a functional *Aprt* message was not transcribed from the *neo*-disrupted allele. Total RNA from D3, MBSF1837, wild-type, and heterozygous liver and lung tissues yielded the expected 3′ amplification product. Neither liver nor lung RNA from homozygous mutant mice produced the wild-type 3′ fragment or a fragment corresponding to any aberrant *Aprt–neo* fusion mRNA (data not shown). This result suggests that the APRT mRNA is either truncated at the *neo* insertion site or that an *Aprt–neo* fusion message is unstable. If a fusion message is unstable, it is unlikely that enough of the mutant APRT subunit is present to form even an unstable dimer with the wild-type subunit. Thus, one would predict 50% of wild-type activity. The fact that only ≈25% of wild-type activity is detected in heterozygous mice suggests that the region involved in subunit dimerization is found in the amino-terminal end of the APRT protein or that other factors are modifying the activity of the remaining APRT enzyme.

Hypoxanthine phosphoribosyltransferase (HPRT) activity was also assayed in erythrocyte lysates of the same mice (data not shown). There is no statistically significant difference between the mean levels of HPRT activity in mice of all three genotypes. This suggests that HPRT activity is not affected by absent or reduced APRT activity. This is in contrast to human HPRT deficiency in which APRT activity in erythrocyte lysates is generally higher than in controls (27).

Characterization of APRT-Deficient Mice. Homozygous mutant mice are usually visually indistinguishable from wild-type and heterozygous littermates before weaning. There are no obvious anatomical defects or behavioral abnormalities. The APRT-deficient mice occasionally have a slightly reduced size and weight when compared with wild-type and heterozygous littermates, but this finding is inconsistent and often disappears as the mouse ages. All APRT-deficient mice excrete larger than normal volumes of colorless to pale yellow urine.

After weaning, the health of ≈35% (22 of 63 mice) of the APRT-deficient mice deteriorates. These mice lose weight and develop a disheveled appearance and hunched posture. Although overtly sick mice may improve briefly, thus far the outcome has been inevitably fatal. Males (16 of 22 mice) are three times more likely to develop these symptoms and die prematurely than females. APRT-deficient mice bred into a C57BL/6J background develop signs of overt illness earlier (3–4 weeks vs. 3–4 months) and die earlier (an average of 75 days vs. an average of 180 days) than a similar proportion of APRT-deficient mice bred into a Black Swiss background.

Table 1. APRT activity of wild-type, heterozygous, and APRT-deficient mice

Aprt genotype	Erythrocyte lysates	Liver extracts
+/+	2.87 ± 1.58 (10)	5.81 ± 4.66 (9)
+/−	0.92 ± 0.28 (14)	1.26 ± 0.36 (6)
−/−	0.02 ± 0.03 (9)	0.03 ± 0.06 (6)

APRT activity is reported in nanomoles of substrate converted per hour per milligram of protein. Numbers represent the mean ± SD. The numbers in parentheses indicate the number of samples assayed. Data from males and females were combined.

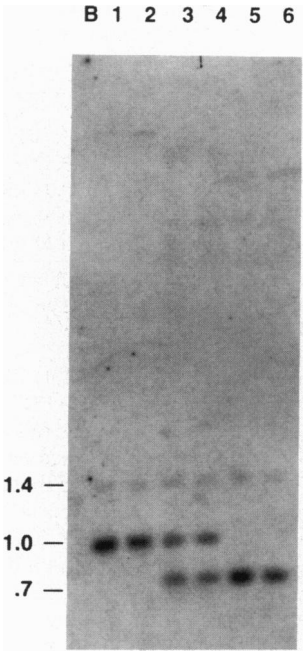

FIG. 2. Southern hybridization of *Bam*HI-digested genomic DNA from *Aprt* ± × *Aprt* ± offspring. Wild-type *Aprt* generates a 1.0-kb fragment, whereas a *neo*-disrupted *Aprt*, which contains an extra *Bam*HI site introduced by *neo*, generates 0.7- and 1.4-kb fragments when hybridized to a probe homologous to *Aprt* exons 3, 4, and 5. The presence of a faint 1.4-kb fragment in the lanes containing wild-type DNA represents nonspecific hybridization since it was not seen in other autoradiograms of the same samples. The sizes of hybridizing fragments are indicated to the left. The blank lane is indicated by B. Lanes 1 and 2 are from wild-type mice; lanes 3 and 4 are from heterozygous mice; and lanes 5 and 6 are from homozygous mutant mice.

In those APRT-deficient mice bred into a C57BL/6J background that are not overtly ill, both males and females have reduced fertility. Matings between homozygous mutant mice have failed to produce viable offspring. Matings between heterozygous mice and mutant mice (male or female) have produced significantly fewer litters and offspring than would normally be expected. Since the mice show appropriate mating behavior and since evidence of mating (i.e., a vaginal plug) has been observed in all crosses, the reduced fertility is unlikely to be the result of a behavioral defect. The production of some viable offspring from heterozygous–homozygous mutant matings suggests that APRT-deficient mice are not inherently sterile.

In contrast, APRT-deficient mice bred into a Black Swiss background are fertile. Matings between homozygous mutant mice produce regularly spaced litters containing an average of 4.2 pups. Coupled with differences in the age at onset of overt illness and death, these data suggest that the genetic background of the mice may have a significant influence on the phenotypic expression of APRT deficiency.

Analysis of Urinary Metabolites. Urine samples from 6-week-old wild-type, heterozygous, and homozygous mutant mice bred into a C57BL/6J background were analyzed for purine metabolites by HPLC. Neither adenine nor DHA was detected in urine samples from wild-type or heterozygous mice. APRT-deficient mice, however, excreted an average of 0.20 ± 0.07 (mean ± SD) mmol of adenine per mmol of creatinine and 0.62 ± 0.32 mmol of DHA per mmol of creatinine. The ratio of adenine/DHA is approximately 1:3, which is significantly higher than the 1:1.5 ratio typically seen in APRT-deficient humans (1). Mass spectrophotometric analysis confirmed that urinary crystals and a stone obtained from the bladder of an APRT-deficient mouse were composed of DHA (data not shown). The amounts of urinary hypoxanthine and xanthine were similar in all three genotypes, but the amount of uric acid excreted by homozygous mutant mice was ≈50% of that excreted by wild-type or heterozygous mice (Table 2). Twelve-week-old homozygous mutant mice excreted amounts of adenine (0.15 ± 0.14 mmol/mmol of creatinine) and DHA (0.43 ± 0.23 mmol/mmol of creatinine) similar to 6-week-old mice. This result suggests that the excretion of adenine metabolites does not change significantly as the mice age.

Urine samples from approximately 4-week-old mice bred into a Black Swiss background were also examined. Wild-type and

Table 2. Urinary metabolites of C57BL/6J and Black Swiss wild-type, heterozygous, and APRT-deficient mice

Background and *Aprt* genotype	Adenine	DHA	Hypo	Xan	Uric acid
C57BL/6J +/+ (6)	<0.01	<0.01	<0.01	<0.01	0.49 ± 0.16
C57BL/6J +/− (5)	<0.01	<0.01	<0.01	0.01 ± 0.01	0.43 ± 0.14
C57BL/6J −/− (4)	0.20 ± 0.07	0.62 ± 0.32	<0.01	<0.01	0.16 ± 0.14
Black Swiss +/+ (3)	<0.01	0.03 ± 0.00	0.02 ± 0.02	0.03 ± 0.02	0.37 ± 0.12
Black Swiss +/− (4)	<0.01	0.01 ± 0.00	0.02 ± 0.01	0.03 ± 0.01	0.38 ± 0.10
Black Swiss −/− (4)	0.80 ± 0.28	0.20 ± 0.03	0.02 ± 0.02	0.05 ± 0.03	0.17 ± 0.07

The concentration of metabolites is reported in millimoles of metabolite per millimole of creatinine. The numbers represent the mean ± SD. The numbers in parentheses indicate the number of mice examined. Data from males and females were combined. Hypo, hypoxanthine; Xan, xanthine.

heterozygous mice did not excrete adenine or DHA (Table 2). DHA crystals, however, were found in the urine of APRT-deficient mice (Fig. 3). Total urinary adenine metabolites (adenine plus DHA, 1.00 ± 0.31 mmol/mmol of creatinine) excreted by the Black Swiss homozygous mutant mice are similar to those excreted by the C57BL/6J APRT-deficient mice. The proportion of adenine (0.80 ± 0.28 mmol/mmol of creatinine) to DHA (0.20 ± 0.03 mmol/mmol of creatinine) excreted, however, is significantly different. The Black Swiss APRT-deficient mice excrete predominantly adenine, which is much more soluble in urine (28) and, consequently, much less deleterious than DHA. Amounts of urinary hypoxanthine, xanthine, and pseudouridine were similar in all three genotypes (Table 2). Amounts of uric acid and uracil were decreased in APRT-deficient mice compared with wild-type or heterozygous mice.

Histopathological Examination of APRT-Deficient Mice. APRT-deficient mice bred into a Black Swiss background were examined beginning at 4 weeks of age. Their kidneys exhibited mild to moderate inflammation and some DHA crystal deposition. By 18–24 weeks of age, parenchymal damage had progressed in severity (Fig. 4). Both intracellular and intratubular crystal formation was noted. Rays of tubular necrosis and regeneration surrounded areas of crystal formation. In some animals, as much as 50–80% of the kidney exhibited severe inflammation and fibrosis of the nephrons. Some (10–20%) of tubules were markedly dilated, but glomeruli, in general, appeared undamaged in both lesioned and normal areas. Both the number and the size of crystals also increased as a function of age, and stones were seen in the renal pelvis, ureter, and urinary bladder. All mice showed signs of proteinaceous material in the lumen of the urinary bladder and/or tubules. One mouse exhibited hematuria. Survival of the mice may be related to two factors: the minimal damage to the glomeruli and the apparent cycling of healthy and damaged areas such that the mice are able to regenerate the damaged tubular epithelium. It is likely that death due to renal failure occurs when the damage ultimately exceeds the rate of repair. Lesions observed in other organs were limited to secondary changes. In the spleens of two 22-week-old mice, there were increased numbers of hemosiderin-laden macrophages, indicative of increased erythrocyte hemolysis. Increased hemolysis is characteristic of the uremia associated with renal failure. In addition, one mouse had multifocal apocellular mineralization in the myocardium, which may also be a consequence of the renal disease. No lesions were seen in age-matched wild-type mice.

APRT-deficient mice bred into a C57BL/6J background were examined at 6 and 12 weeks of age. These mice showed the same kidney pathology as the Black Swiss mice except that the progression of the interstitial fibrosis was more rapid. At 6 weeks of age, as much as 20–30% of each kidney was inflamed and necrotic, and by 12 weeks of age, as much as 70–80% of each kidney was involved. In moribund mice, the severity of the kidney histopathology correlates well with the observed age at onset of symptoms and the average age of death.

DISCUSSION

APRT-deficient mice, produced by gene targeting in ES cells, excrete adenine and DHA and develop crystalluria and kidney stones. Thus, these mice exhibit all of the characteristics typically associated with human APRT deficiency. This is in

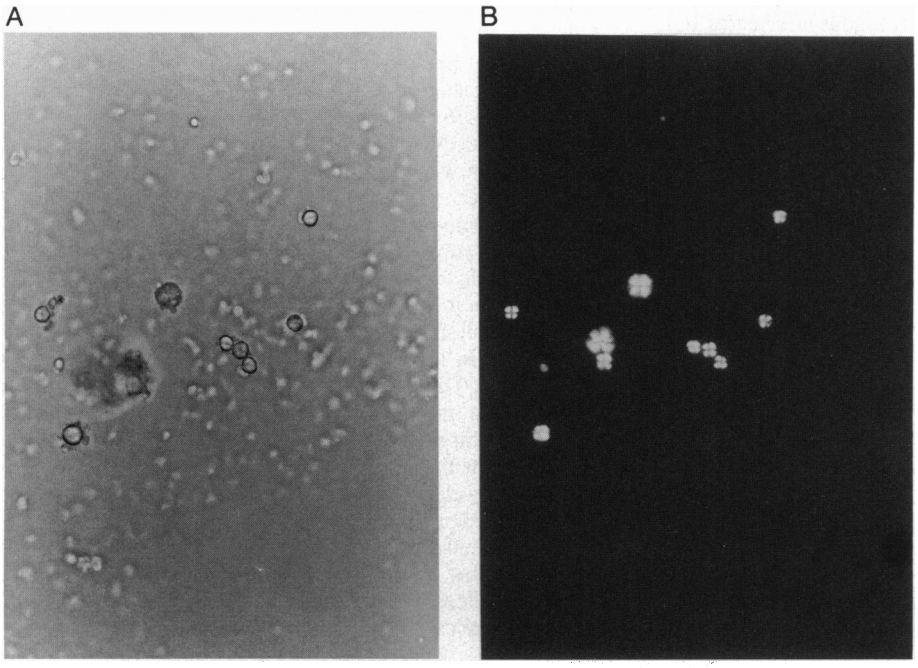

FIG. 3. DHA crystals in urine of APRT-deficient mice. (*A*) Magnified bright-field view of urinary DHA crystals obtained from a 4-week-old Black Swiss APRT-deficient mouse. (*B*) Dark-field view of crystals pictured in *A*, visualized with a polarized light source.

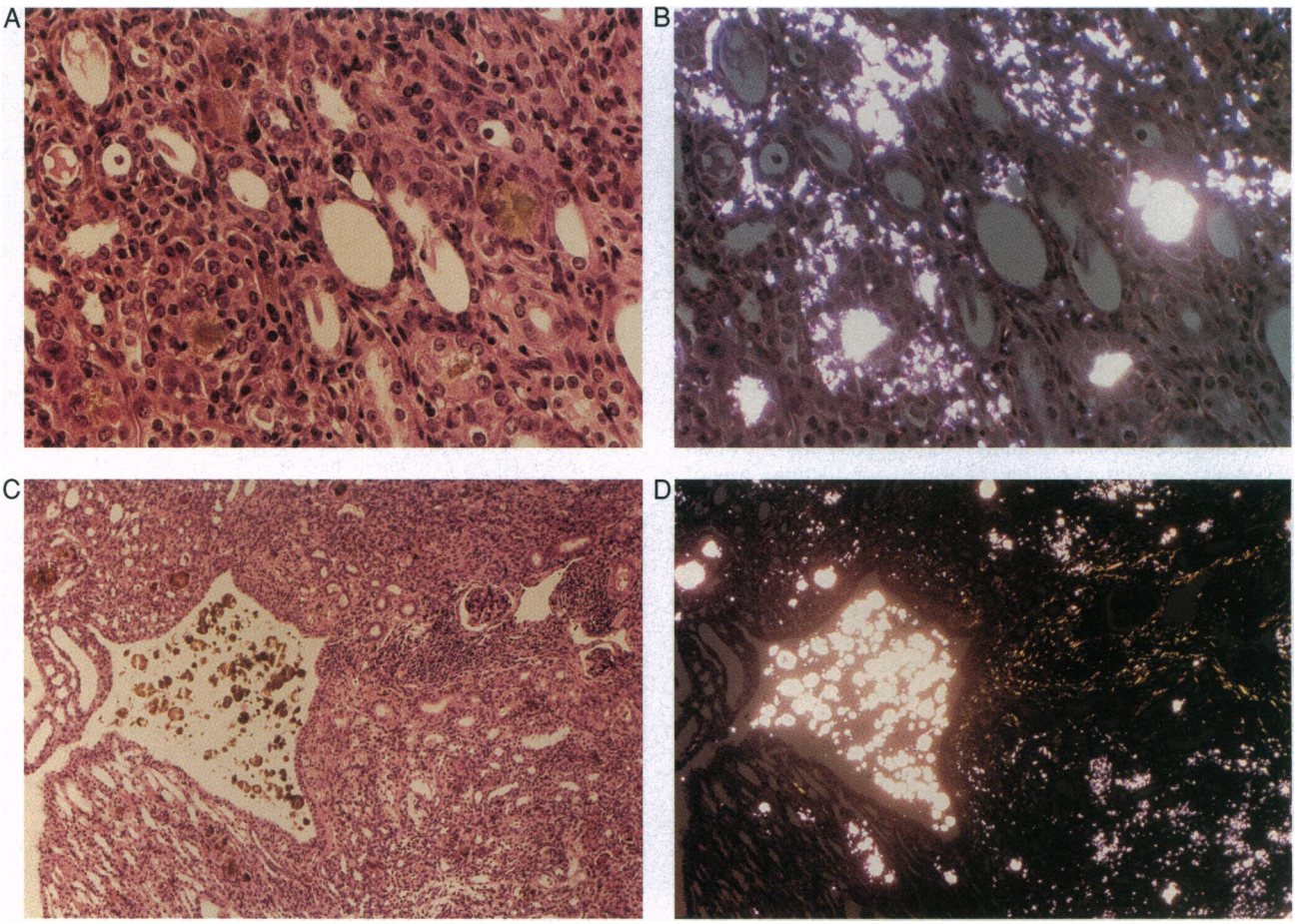

FIG. 4. Kidney histopathology. (*A*) Bright-field view of a hemotoxylin- and eosin-stained histological section from an approximately 3-month-old Black Swiss APRT-deficient male mouse. Note the large, rosette-shaped, brown-yellow crystals. (*B*) Dark-field view of *A*, visualized with a polarized light source. (*C*) Bright-field view of another histological section from the same mouse kidney pictured in *A*. Note the accumulation of stones in the renal pelvis. (*D*) Dark-field view of section in *C*, visualized with a polarized light source. (×94.)

contrast to other attempts to use ES cells to produce mouse models of purine metabolic disorders. Mice deficient in HPRT activity, for example, do not exhibit any of the significant characteristics of Lesch–Nyhan syndrome (29, 30). HPRT, therefore, appears to play a somewhat different role in mouse/purine homeostasis than it does in humans. Adenosine deaminase, on the other hand, appears to play a more critical role in murine than in human fetal development (31, 32). Human adenosine deaminase deficiency results in severe combined immunodeficiency disease characterized by the absence of both T and B lymphocytes. Adenosine deaminase-deficient mice, however, have approximately normal numbers of thymocytes but die perinatally from severe liver cell degeneration, which is not seen in the human disorder. The similar phenotype of APRT-deficient mice and humans suggests that the function and importance of APRT are quite similar in mouse and man. This makes the APRT-deficient mouse model particularly useful for understanding the human disease.

As human and mouse APRT deficiencies appear similar in most respects, the observation of the expected number of each genotype from a cross of heterozygous mice suggests that observation of fewer than the expected numbers of APRT-deficient humans, based on the observed population frequency of heterozygotes, may not be a consequence of *in utero* lethality, as previously hypothesized (1, 13). Recent studies in which 10,000 or 160,000 kidney stones from two Caucasian populations were analyzed identified only 14 and 3 DHA stones, respectively (33, 34). Since the frequency of DHA stones was approximately equal to the observed frequency of APRT deficiency in these populations, misdiagnosis, a significant problem in the past, may no longer contribute to the discrepancy between the numbers of expected and identified homozygotes. The remaining alternative is that there is a large population of asymptomatic, homozygous mutant individuals. It has been estimated from surveys of the families of symptomatic APRT-deficient patients that ≈15% of APRT-deficient individuals are clinically asymptomatic, aside from the excretion of adenine and DHA (1). In both the C57BL/6J and Black Swiss background mice, only ≈33% of the homozygous mutant mice die prematurely because of a lack of renal function. Thus, it is possible that the majority of APRT-deficient humans are asymptomatic or only mildly affected. Ascertainment bias could be responsible for the belief that ≈85% of homozygous mutant humans have overt kidney stone formation.

The observed differences in adenine metabolism in the two genetic backgrounds of APRT-deficient mice suggest that the introduction of the disrupted *Aprt* into inbred mouse strains may elucidate other factors that influence adenine metabolism, stone formation, or kidney function. Phenotypic variation in human APRT deficiency has been well documented (1). The age at onset and severity of clinical symptoms are known to vary even among siblings who carry the same gene defect(s) (35). It is likely that mouse strain variations in *de novo* purine synthesis, polyamine synthesis, other purine metabolic enzymes, and kidney functions such as the ability to supersaturate the urine, may have a significant influence on stone formation or disease progression. The ability to generate different inbred strains carrying the disrupted *Aprt*, to establish informative matings and analyze the offspring at the biochemical and molecular levels, should allow one to identify those specific enzymes or genes that influence the APRT-deficient phenotype. These studies may be of importance

in understanding why some APRT-deficient individuals remain asymptomatic their entire lives, whereas others have early and rapid progression to end-stage renal failure.

Strain-specific differences in XDH may explain some of the variation observed between the two different APRT-deficient mouse backgrounds. XDH converts hypoxanthine to xanthine and xanthine to uric acid (36, 37). It is the rate-limiting enzyme in purine degradation and may regulate the balance between degradation and salvage of purines. Unlike humans, whose XDH is confined to the liver and intestinal mucosa, mice express XDH activity in a variety of tissues. Mouse erythrocytes have been reported to contain XDH that varies approximately five-fold between different mouse strains (38). Variation in the age at which adult levels of the enzyme activity are attained has also been reported (39, 40). C57BL/6J APRT-deficient mice, in contrast to Black Swiss mice, may have higher levels of XDH activity, earlier expression of adult levels of XDH activity, or an XDH enzyme variant with a higher affinity for adenine. Any of these possibilities could lead to increased conversion of adenine to DHA. It is likely that the higher DHA excretion exhibited by the C57BL/6J APRT-deficient mice leads to the more rapid progression of the kidney disease.

The role of XDH in determining the phenotypic expression of APRT deficiency is supported by experience gained in the treatment of the human disease with allopurinol. Allopurinol, an XDH inhibitor, mitigates the kidney disease by increasing the excretion of adenine relative to DHA (41). Total excretion of adenine metabolites is unaffected. This pharmacologic effect may provide a mechanistic clue to the observed differences in the C57BL/6J and Black Swiss APRT-deficient mice.

In addition to the utility of APRT-deficient mice as a model for human APRT deficiency, these mice offer a unique opportunity to study the early changes in kidney function leading to stone formation and renal failure. Kidney stones and renal failure are common clinical disorders associated with significant morbidity (42, 43). Relatively little is known, however, about the changes that predispose a kidney to develop stones, and current animal models of renal failure induced by acute surgical, pharmacological, or immunological traumas do not mimic renal failure as it typically develops in humans (44–46). Results presented here indicate that APRT-deficient mice predictably and spontaneously develop stones and, eventually, renal failure. This model may enable a detailed investigation of the subtle changes and factors predisposing to stone formation and renal failure.

We thank Dr. T. Doetschman for his assistance, Dr. L. Bowers for mass spectrophotometric analysis of stones, and the personnel of the Division of Comparative Pathology, University of Cincinnati, for their help in preparing samples for histological examination. This work was supported by National Institutes of Health Grants DK38185, ES05652, and ES06096.

1. Simmonds, H. A., Sahota, A. S. & Van Acker, K. J. (1995) in *The Metabolic and Molecular Bases of Inherited Disease*, eds. Scriver, C. R., Beaudet, W. S., Sly, W. S. & Valle, D. (McGraw–Hill, New York), pp. 1707–1724.
2. Williams-Ashman, H. G., Seidenfeld, J. & Galletti, P. (1982) *Biochem. Pharmacol.* **31,** 277–288.
3. Montero, C., Smolenski, R. T., Duley, J. A. & Simmonds, H. A. (1990) *Biochem. Pharmacol.* **40,** 2617–2623.
4. Wyngaarden, J. B. & Dunn, J. T. (1957) *Arch. Biochem. Biophys.* **70,** 150–156.
5. Peck, C. C., Bailey, F. J. & Moore, G. L. (1977) *Transfusion* **17,** 383–390.
6. Glicklich, D., Gruber, H. E., Matas, A. J., Tellis, V. A., Karwa, G., Finley, K., Salem, C., Soberman, R. & Seegmiller, J. E. (1988) *Q. J. Med.* **69,** 785–793.
7. Fye, K. H., Sahota, A. S., Hancock, D. C., Gelb, A. B., Chen, J., Sparks, J. W., Sibley, R. K. & Tischfield, J. A. (1993) *Arch. Intern. Med.* **153,** 767–770.
8. Frantini, A., Simmers, R. N., Callen, D. F., Hyland, V. J., Tischfield, J. A., Stambrook, P. J. & Sutherland, G. R. (1986) *Cytogenet. Cell Genet.* **43,** 10–13.
9. Sahota, A., Chen, J., Behzadian, M. A., Ravindra, R., Takeuchi, H., Stambrook, P. J. & Tischfield, J. A. (1991) *Am. J. Hum. Genet.* **48,** 983–989.
10. Fox, I. H., Lacroix, S., Planet, G. & Moore, M. (1977) *Medicine* **56,** 515–526.
11. Emmerson, B. T., Johnson, C. A. & Gordon, R. B. (1976) *J. Clin. Chem. Clin. Biochem.* **14,** 285–290.
12. Kamatani, N., Terai, C., Kuroshima, S., Nishioka, K. & Mikanagi, K. (1987) *Hum. Genet.* **75,** 163–168.
13. Van Acker, K. J., Simmonds, H. A., Potter, C. & Cameron, J. S. (1977) *N. Engl. J. Med.* **297,** 127–132.
14. Devenuto, F., Wilson, S. M., Billings, T. A. & Shields, C. E. (1976) *Transfusion* **16,** 24–31.
15. Bartlett, G. R. (1977) *Transfusion* **17,** 351–357.
16. Bartlett, G. R. (1977) *Transfusion* **17,** 367–373.
17. Ericson, A., Groth, T., Niklasson, F. & de Verdier, C. H. (1980) *Scan. J. Clin. Lab. Invest.* **40,** 1–8.
18. Doetschman, T., Eistetter, H., Katz, M., Schmidt, W. & Kemler, R. (1985) *J. Embryol. Exp. Morphol.* **87,** 27–45.
19. Robertson, E. J. (1987) in *Teratocarcinomas and Embryonic Stem Cells: A Practical Approach*, ed. Robertson, E. J. (IRL, Washington, DC), pp. 71–112.
20. Hogan, B., Constantini, F. & Lacy, E. (1986) *Manipulating the Mouse Embryo: A Laboratory Manual* (Cold Spring Harbor Lab. Press, Plainview, NY).
21. Mullenbach, R., Lagoda, P. J. & Welter, C. (1989) *Trends Genet.* **5,** 391.
22. Sambrook, J., Fritsch, E. F. & Maniatis, T. (1989) *Molecular Cloning: A Laboratory Manual* (Cold Spring Harbor Lab. Press, Plainview, NY), 2nd Ed.
23. Dush, M. K., Sikela, J. M., Khan, S. A., Tischfield, J. A. & Stambrook, P. J. (1985) *Proc. Natl. Acad. Sci. USA* **82,** 2731–3735.
24. Simmonds, H. A., Duley, J. A. & Davies, P. M. (1991) in *Techniques in Diagnostic Human Biochemical Genetics: A Laboratory Manual*, ed. Hommes, F. A. (Wiley–Liss, London), pp. 397–425.
25. Mansour, S. L., Thomas, K. R. & Capecchi, M. R. (1988) *Nature (London)* **336,** 348–352.
26. Wilson, J. M., Daddona, P. E., Simmonds, H. A., Van Acker, K. J. & Kelley, W. N. (1982) *J. Biol. Chem.* **257,** 1508–1515.
27. Rossiter, B. J. F. & Caskey, C. T. (1995) in *The Metabolic and Molecular Bases of Inherited Disease*, eds. Scriver, C. R., Beaudet, W. S., Sly, W. S. & Valle, D. (McGraw–Hill, New York), pp. 1679–1706.
28. Moore, G. L. & Ledford, M. E. (1975) *Biochem. Med.* **14,** 147–151.
29. Hooper, M., Hardy, K., Handyside, A., Hunter, S. & Monk, M. (1987) *Nature (London)* **326,** 292–295.
30. Kuehn, M. R., Bradley, A., Roberston, E. J. & Evans, M. J. (1987) *Nature (London)* **236,** 295–298.
31. Migchielsen, A. A. J., Breuer, M. L., van Roon, M. A., te Riele, H., Zurcher, C., Ossendorp, F., Toutain, S., Hershfield, M. S., Berns, A. & Valerio, D. (1995) *Nat. Genet.* **10,** 279–287.
32. Wakaniya, M., Blackburn, M. R., Jurecic, R., McArthur, M. J., Geske, R. S., Cartwright, J., Jr., Mitani, K., Vaishnav, S., Belmont, J. W. & Kellems, R. E. (1995) *Proc. Natl. Acad. Sci. USA* **92,** 3673–3677.
33. Ceballos-Picot, I., Perignon, J. L., Hamet, M., Daudon, M. & Kamoun, P. (1992) *Lancet* **339,** 1050–1051.
34. Gleeson, M. J. & Griffith, D. P. (1989) *J. Urol.* **142,** 834.
35. Sahota, A., Chen, J., Boyadjiev, S. A., Gault, M. H. & Tischfield, J. A. (1994) *Hum. Mol. Genet.* **3,** 817–818.
36. Kooj, A. (1994) *Histochem. J.* **26,** 889–915.
37. Parks, D. A. & Granger, D. N. (1986) *Acta Physiol. Scand. Suppl.* **548,** 87–99.
38. Henderson, J. F., Zombor, G., Johnson, M. M. & Smith, C. M. (1983) *Comp. Biochem. Physiol. B* **76,** 419–422.
39. Lee, P. C. (1973) *Dev. Biol.* **31,** 227–257.
40. Manchester, K. A. & Amy, N. K. (1988) *J. Biochem.* **20,** 1061–1066.
41. Smith, G. W. (1987) *Br. J. Clin. Pract.* **41,** 710–711.
42. Smith, L. H. (1989) *J. Urol.* **141,** 707–710.
43. Soyannwo, M. A. (1993) *Am. J. Kidney Dis.* **22** (Suppl. 2), 21–29.
44. Consensus Conference (1989) *J. Urol.* **141,** 804–808.
45. Strauch, M. & Gretz, N. (1988) *Contrib. Nephrol.* **60,** 1–8.
46. Gretz, N., Meisinger, E. & Strauch, M. (1988) *Contrib. Nephrol.* **60,** 252–263.